Pergamon

Int. J. Solids Structures Vol. 31, No. 17, pp 2377–2391, 1994

0020–7683/94 $7.00 + .00

0020–7683(94)E0029–U

VIBRATION ANALYSIS OF A PARTIALLY COVERED DOUBLE SANDWICH CANTILEVER BEAM WITH CONCENTRATED MASS AT THE FREE END

Q. CHEN and C. LEVY†
Department of Mechanical Engineering, Florida International University, Miami, FL 33199, U.S.A.

(*Received* 28 *September* 1993; *in revised form* 15 *December* 1993)

Abstract—A cantilever beam, partially covered by damping and constraining layers, with concentrated mass at the free end is studied. Euler beam theory is employed to derive the equations of motion of the system and the resonant frequency and loss factor of the system are analysed. The resonant frequency and system loss factor for different geometrical and physical parameters are determined. Variation of these two parameters are found to strongly depend on the geometrical and physical properties of the constraining layers and the mass ratio.

NOMENCLATURE

A_i	cross-sectional area of layer i
A_{c1}, A_{c2}	cross-sectional area of the damping layers
B_1	$(1/EA)(E_3A_3+A_4A_4)$
B_2	E_3A_3/EA
B_3	E_4A_4/EA
B_4	$(1/EA)[(E_1A_1+E_4A_4)h_{02}-E_1A_1h_{01}]$
B_5	$(E_1A_1h_{01}+E_3A_3h_{02})/EA$
B_6	$(E_1A_1+E_3A_3)/EA$
B_7	$B_1h_{01}-B_2h_{02}$
B_8	$(E_1A_1+E_4A_4)/EA$
D	$b[E_1h_1^3+E_3h_3^3+E_4h_4^3]/12$
D_{t1}	$\frac{1}{12}E_1h_1^3$ bending rigidity of the original beam
EA	$E_1A_1+E_3A_3+E_4A_4$
E_i	Young modulus of the ith layer
G_{ci}^*	complex modulus of the ith layer, $G_{ci}^*=G_{ci}(1+j\eta_{ci})$
h_i	thickness of the ith layer
h_{c1}, h_{c2}	thickness of the damping layers
h_{01}	$h_{c2}+\frac{1}{2}(h_1+h_4)$
h_{02}	$h_{c1}+h_{c2}+h_1+\frac{1}{2}(h_3+h_4)$
j	$\sqrt{-1}$
k_n^*	complex characteristic value
L	length of the beam
L_1	length of the damping coverage
M_1, M_2	bending moment at $x=0$ and $x=L_1$, respectively
M_0	attached mass at the free end
M	mass of primary beam and, if covered, constraining and damping layers
m	mass density per unit length of section 1
P_i	axial force of the ith layer
S_1, S_2	shear force
t	time
u_i	axial displacement of the ith layer
w_1, w_2	transverse displacements of sections 1 and 2, respectively
x	axial or longitudinal coordinate
γ_{ci}	core shear deformation of the ith layer
η	system loss factor
η_{ci}	core loss factor of the ith layer
ρ_i	mass density of the ith layer material
Ω	natural frequency of the system
Ω^*	complex natural frequency, $\Omega^*=\Omega(1+j\eta)^{1/2}$.

† All correspondence should be addressed to Dr Levy at the above address.

INTRODUCTION

The vibration problem of a beam carrying a concentrated mass or concentrated masses and having arbitrary boundary conditions at the end supports is of great interest to the practical engineer (Magrab, 1979). For example, this system may be considered as a model of a robot arm with a mass in its end effector. The vibrational aspects of this kind of system may be of great interest when, due to some motion at the shoulder joint, the system is made to oscillate. Rao (1990) discussed the cantilever Euler beam with concentrated tip mass as one of the examples in his book. Pan (1965) studied the transverse vibration of an Euler beam carrying a system of heavy bodies. Rami Reddy and Amba-Rao (1973) solved the problem of vibrations of beams with non-classical boundary conditions (rotational and translational springs at the supports) using transfer matrices. Amba-Rao and Hussaini (1975) obtained a closed-form solution for the classical problem of a beam carrying masses. The dynamic properties of structures carrying concentrated masses were studied by Laura *et al.* (1977, 1987). Stokey and Zorowski (1959) solved the normal vibrations of a uniform plate carrying any number of finite masses. An approximate method to find the fundamental frequency of a restrained cantilever beam carrying a tip heavy body was presented by Gurgoze (1986).

As a means of reducing this vibration, the beam may be covered by a viscoelastic material. The use of viscoelastic materials as means of increasing energy loss in beams and plates under flexural vibrations has been investigated by many authors. For example, Rao (1978) and Ditaranto (1965) obtained differential equations of motion for a sandwich beam, while Yan and Dowell (1972) found the equations of motion for sandwich plates. The effects of different boundary conditions were also studied in Rao (1978) and short beams were investigated by Rao (1977). Mead and Markus (1969) studied the forced vibrations of damped fully covered sandwich beams. Lall *et al.* (1988) studied the damping characteristics of partially covered sandwich beams. A summary of work involving sandwich structures is found in Chen (1986).

Even though cantilever beams with tip masses have been scrutinized extensively and beams with full and partial damping coverage on one lateral surface have been discussed, no papers have discussed the effect of tip mass on the partially covered double sandwich cantilever beam. Levy and Chen (1994) presented an analysis of the double, sandwich-type cantilever beam covered with a viscoelastic material. The model developed in that investigation will be employed, except that a mass at the end of the beam will be added. In this paper, the partially covered double sandwich cantilever with concentrated mass at the free end is studied. The equations of motion for the system are derived and the resonant frequency and system loss factor for different geometrical and physical parameters are also discussed. It is known that the damping material's material parameters are functions of temperature and, therefore, affects the frequency of vibration. However, in a normal factory environment, variation of temperature is small; thus, the damping material's material parameters will be considered constant in this study.

EQUATIONS OF MOTION

The double sandwich cantilever with concentrated mass at the free end is shown in Fig. 1. To make the mathematical method tractable, the following assumptions are made in the analysis:

(1) the beam deflection is small and uniform across any section;
(2) the primary beam and the upper and lower constraining beams are assumed to be isotropic;
(3) the longitudinal and rotatory inertia effects at the beam are neglected;
(4) the damping layers which carry shear but no direct stress are assumed to be linear viscoelastic;
(5) no slip occurs at the interface between the layers;
(6) the mass at the end effector can be modeled as a concentrated mass.

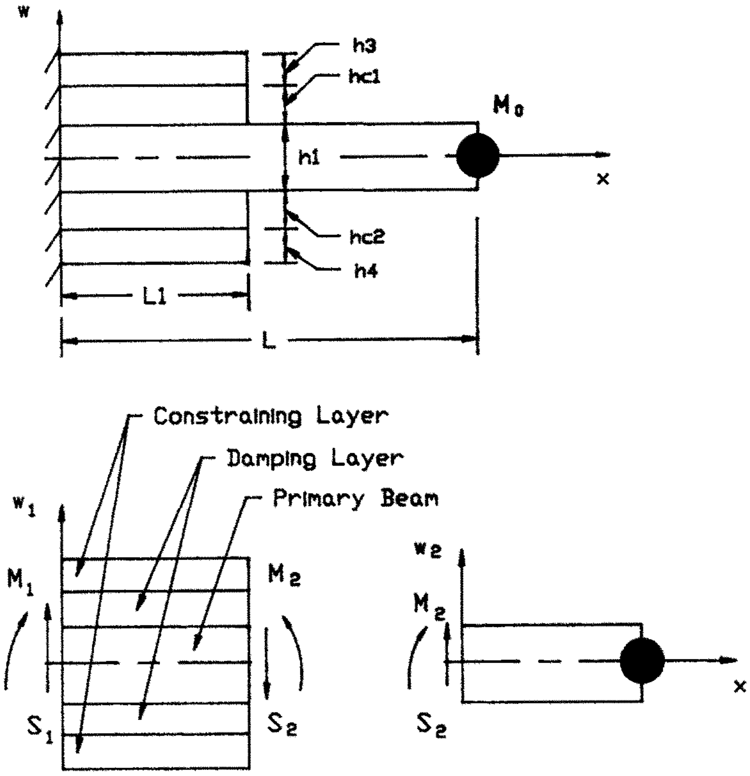

Fig. 1. Model of the double sandwich cantilever beam with tip mass.

The beam is separated into two sections; section 1 is a double sandwich-type beam containing the damping and constraining layers, and section 2 is the ordinary beam with mass M_0 at its right end. Matching conditions at the interface of the two sections will be applied on the transverse displacement, the rotation, and the shear force and moment continuity. The mass of the beam per unit length for section 2 may be expressed as

$$m_{20} = m_2 + M_0\delta(x-L), \tag{1}$$

where m_2 is the mass per unit length of the uncovered portion of the beam, and $\delta(x-L)$ is the Dirac delta function. Hence, the differential equation of motion for section 2 is

$$D_{t1}\frac{\partial^4 w_2}{\partial x^4} + [m_2 + M_0\delta(x-L)]\frac{\partial^2 w_2}{\partial t^2} = 0, \tag{2}$$

where $D_{t1} = E_1 h_1^3 b/12$ is the bending stiffness. The boundary conditions at $x = L_1$ for section 2 are

$$D_{t1}\frac{\partial^2 w_2}{\partial x^2} - M_2 = 0 \tag{3a}$$

$$D_{t1}\frac{\partial^3 w_2}{\partial x^3} + S_2 = 0. \tag{3b}$$

Since the effect of the mass is taken into account in eqn (2), the boundary conditions at $x = L$ are

$$D_{t1}\frac{\partial^2 w_2}{\partial x^2}=0 \tag{3c}$$

$$D_{t1}\frac{\partial^3 w_2}{\partial x^3}=0. \tag{3d}$$

The differential equations of motion for section 1 are obtained by minimizing the variation in the total energy of the section. The equations are given in Levy and Chen (1994) as

$$\begin{bmatrix} a_{11} & a_{12} & a_{13} \\ a_{21} & a_{22} & a_{23} \\ a_{31} & a_{32} & a_{33} \end{bmatrix} \begin{bmatrix} w_1 \\ \gamma_{c1} \\ \gamma_{c2} \end{bmatrix} = \{0\}, \tag{4}$$

where the a_{ij}s are given as follows:

$$a_{11}=m\frac{\partial^2}{\partial t^2}+(D+E_1A_1B_7^2+E_3A_3B_4^2+E_4A_4B_2B_5^2)\frac{\partial^4}{\partial x^4}$$

$$a_{12}=+(E_1A_1B_2B_7-E_3A_3B_4B_8+E_4A_4B_2B_5)h_{c1}\frac{\partial^3}{\partial x^3}$$

$$a_{13}=(-E_1A_1B_3B_7-E_3A_3B_3B_4+E_4A_4B_5B_6)h_{c2}\frac{\partial^3}{\partial x^3}$$

$$a_{21}=(E_1A_1B_2B_7-E_3A_3B_4B_8+E_4A_4B_2B_5)h_{c1}\frac{\partial^3}{\partial x^3}$$

$$a_{22}=(B_2^2E_1A_1+B_8^2E_3A_3+B_2^2E_4A_4)h_{c1}^2\frac{\partial^2}{\partial x^2}-G_{c1}A_{c1}$$

$$a_{23}=(-E_1A_1B_2B_3+E_3A_3B_3B_8+E_4A_4B_2B_6)h_{c1}h_{c2}\frac{\partial^2}{\partial x^2}$$

$$a_{31}=(E_4A_4B_5B_6-E_1A_1B_3B_7-E_3A_3B_3B_4)h_{c1}h_{c2}\frac{\partial^3}{\partial x^3}$$

$$a_{32}=(E_3A_3B_3B_8-E_1A_1B_2B_3+E_4A_4B_2B_6)h_{c1}h_{c2}\frac{\partial^2}{\partial x^2}$$

$$a_{33}=(E_1A_1B_3^2+E_3A_3B_3^2+E_4A_4B_6^2)h_{c2}^2\frac{\partial^2}{\partial x^2}-G_{c2}A_{c2}. \tag{4a–i}$$

The corresponding boundary conditions generated from the variation of total energy are

$$(D+E_1A_1B_7^2+E_3A_3B_4^2+E_4A_4B_5^2)\frac{\partial^2 w_1}{\partial x^2}+(E_1A_1B_2B_7-E_3A_3B_4B_8+E_4A_4B_2B_5)h_{c1}\frac{\partial \gamma_{c1}}{\partial x}$$
$$+(E_4A_4B_5B_6-E_1A_1B_3B_7-E_3A_3B_3B_4)h_{c2}\frac{\partial \gamma_{c2}}{\partial x}-M_1=0 \quad \text{or} \quad \frac{\partial w_1}{\partial x}=0 \tag{5a}$$

$$(D+E_1A_1B_7^2+E_3A_3B_4^2+E_4A_4B_5^2)\frac{\partial^3 w_1}{\partial x^3}+(E_1A_1B_2B_7-E_3A_3B_4B_8+E_4A_4B_2B_5)h_{c1}\frac{\partial^2 \gamma_{c1}}{\partial x^2}$$
$$+(E_4A_4B_5B_6-E_1A_1B_3B_7-E_3A_3B_3B_7)h_{c2}\frac{\partial^2 \gamma_{c2}}{\partial x^2}+S_1=0 \quad \text{or} \quad w_1=0 \tag{5b}$$

$$(E_3A_3B_4B_8-E_1A_1B_2B_7-E_4A_4B_2B_5)h_{c1}\frac{\partial^2 w_1}{\partial x^2}-(E_1A_1B_2^2+E_3A_3B_8^2+E_4A_4B_2^2)h_{c1}^2\frac{\partial\gamma_{c1}}{\partial x}$$

$$+(E_1A_1B_2B_3-E_3A_3B_3B_8-E_4A_4B_2B_6)h_{c1}h_{c2}\frac{\partial\gamma_{c2}}{\partial x}=0 \quad \text{or} \quad \gamma_{c1}=0 \qquad (5c)$$

$$(E_1A_1B_3B_7+E_3A_3B_3B_4-E_4A_4B_5B_6)h_{c2}\frac{\partial^2 w_1}{\partial x^2}$$

$$+(E_1A_1B_2B_3-E_3A_3B_3B_8-E_4A_4B_2B_6)h_{c1}h_{c2}\frac{\partial\gamma_{c1}}{\partial x}$$

$$-(E_1A_1B_3^2+E_3A_3B_3^2+E_4A_4B_6^2)h_{c2}^2\frac{\partial\gamma_{c2}}{\partial x}=0 \quad \text{or} \quad \gamma_{c2}=0. \qquad (5d)$$

Here, w_1 represents the displacement in section 1, and the remaining symbols used in eqns (4)–(5) are defined in the Nomenclature.

Hence, the boundary conditions at $x = 0$ are

$$w_1 = 0 \qquad (6a)$$

$$\frac{\partial w_1}{\partial x} = 0 \qquad (6b)$$

$$\gamma_{c1} = 0 \qquad (6c)$$

$$\gamma_{c2} = 0. \qquad (6d)$$

At $x = L_1$, the interface between damped and undamped parts of the beam, geometric continuity and generalized force continuity must apply, namely

$$w_1 = w_2 \qquad (7a)$$

$$\frac{\partial w_1}{\partial x} = \frac{\partial w_2}{\partial x} \qquad (7b)$$

$$M_1 = M_2 \qquad (7c)$$

$$S_1 = S_2. \qquad (7d)$$

Also, by using eqns (3a, b), (5a–d), and (7a–d), we obtain the conditions:

at $x = L_1$:

$$(D+E_1A_1B_7^2+E_3A_3B_4^2+E_4A_4B_5^2)\frac{\partial^2 w_1}{\partial x^2}+(E_1A_1B_2B_7-E_3A_3B_4B_8+E_4A_4B_2B_5)h_{c1}\frac{\partial\gamma_{c1}}{\partial x}$$

$$+(E_4A_4B_5B_6-E_1A_1B_3B_7-E_3A_3B_3B_4)h_{c2}\frac{\partial\gamma_{c2}}{\partial x}+D_{t1}\frac{\partial^2 w_2}{\partial x^2}=0 \qquad (8a)$$

$$(D+E_1A_1B_7^2+E_3A_3B_4^2+E_4A_4B_5^2)\frac{\partial^3 w_1}{\partial x^3}+(E_1A_1B_2B_7-E_3A_3B_4B_8+E_4A_4B_2B_5)h_{c1}\frac{\partial^2\gamma_{c1}}{\partial x^2}$$

$$+(E_4A_4B_5B_6-E_1A_1B_3B_7-E_3A_3B_3B_4)h_{c2}\frac{\partial^2\gamma_{c2}}{\partial x^2}+D_{t1}\frac{\partial^3 w_2}{\partial x^3}=0 \qquad (8b)$$

$$(E_3A_3B_4B_8-E_1A_1B_2B_7-E_4A_4B_2B_5)h_{c1}\frac{\partial^2 w_1}{\partial x^2}-(E_1A_1B_2^2+E_3A_3B_8^2+E_4A_4B_2^2)h_{c1}^2\frac{\partial\gamma_{c1}}{\partial x}$$

$$+(E_1A_1B_2B_3-E_3A_3B_3B_8-E_4A_4B_2B_6)h_{c1}h_{c2}\frac{\partial\gamma_{c2}}{\partial x}=0 \qquad (8c)$$

$$(E_1A_1B_3B_7+E_3A_3B_3B_4-E_4A_4B_5B_6)h_{c2}\frac{\partial^2 w_1}{\partial x^2}+(E_1A_1B_2B_3-E_3A_3B_3B_8-E_4A_4B_2B_6)$$
$$\times h_{c1}h_{c2}\frac{\partial \gamma_{c1}}{\partial x}-(E_1A_1B_3^2+E_3A_3B_3^2+E_4A_4B_6^2)h_{c2}^2\frac{\partial \gamma_{c2}}{\partial x}=0. \quad (8d)$$

RESONANT FREQUENCY AND LOSS FACTOR

As part of the design process of a partially covered, double sandwich-type cantilever beam, one will normally be interested in the resonant frequencies and loss factors in the first few modes of vibrations (Rao, 1978). To obtain the resonant frequencies and loss factors, assume the displacement solution of section 2 to be in the form

$$w_2(x,t) = W_2(x)\,\mathrm{e}^{i\Omega^* t}. \quad (9)$$

For mass M_0 attached at $x=\xi$, substituting eqn (9) into eqn (2) gives

$$\frac{d^4W_2(x)}{dx^4}-\frac{\omega^4}{L_2^4}\left[1+\frac{M_0}{m_0}L_2\delta(x-\xi)\right]W_2(x)=0, \quad (10)$$

where $m_0 = m_2L_2$, $L_2 = L-L_1$, $c_0^4 = D_{t1}/m_2$, and $\omega^2 = \Omega^* L_2^2/c_0^2$. Taking the Laplace transform eqn (10) with respect to the variable x yields

$$\bar{W}_2(s) = \left[s^3W_2(L_1)+s^2W_2'(L_1)+sW_2''(L_1)+W_2'''(L_1)+\frac{\omega^4}{L_2^3}\frac{M_0}{m_0}\mathrm{e}^{-\xi s}W_2(\xi)\right]\bigg/\left(s^4-\frac{\omega^4}{L_2^4}\right), \quad (11)$$

where s represents the transform variable and the first four terms give contributions due to the boundary condition. Taking the inverse transform of eqn (11), we obtain

$$W_2(x) = W_2(\xi)\left\{\hat{W}_2(L_1)U\left(\frac{\omega x}{L_2}\right)+\hat{W}_2'(L_1)\left(\frac{L_2}{\omega}\right)V\left(\frac{\omega x}{L_2}\right)+\hat{W}_2''(L_1)\left(\frac{L_2}{\omega}\right)^2S\left(\frac{\omega x}{L_2}\right)\right.$$
$$\left.+\hat{W}_2'''(L_1)\left(\frac{L_2}{\omega}\right)^3T\left(\frac{\omega x}{L_2}\right)+\frac{M_0}{m_0}\omega T\left[\frac{\omega(x-\xi)}{L_2}\right]H(x-\xi)\right\}, \quad (12)$$

where

$$\hat{W}_2^{(j)}(L_1) = W_2^{(j)}(L_1)/W_2(\xi),$$
$$U(x) = \tfrac{1}{2}[\cos(x)+\cosh(x)],$$
$$V(x) = \tfrac{1}{2}[\sin(x)+\sinh(x)],$$
$$S(x) = \tfrac{1}{2}[\cosh(x)-\cos(x)],$$
$$T(x) = \tfrac{1}{2}[\sinh(x)-\sin(x)],$$

and $H(x)$ is the Heaviside step function. Since the solution must hold at $x=\xi$, eqn (12) yields the following form of the frequency equation

$$\hat{W}_2(L_1)U\left(\frac{\omega_n\xi}{L_2}\right)+\hat{W}'_2(L_1)\left(\frac{L_2}{\omega_n}\right)V\left(\frac{\omega_n\xi}{L_2}\right)+\hat{W}''_2(L_1)\left(\frac{L_2}{\omega_n}\right)^2 S\left(\frac{\omega_n\xi}{L_2}\right)$$
$$+\hat{W}'''_2(L_1)\left(\frac{L_2}{\omega_n}\right)^3 T\left(\frac{\omega_n\xi}{L_2}\right)=1. \quad (13)$$

The corresponding eigenfunction is:

$$W_{2n}(x)=\hat{W}_{2n}(L_1)U\left(\frac{\omega_n x}{L_2}\right)+\hat{W}'_{2n}(L_1)\left(\frac{L_2}{\omega_n}\right)V\left(\frac{\omega_n x}{L_2}\right)+\hat{W}''_{2n}(L_1)\left(\frac{L_2}{\omega_n}\right)^2 S\left(\frac{\omega_n x}{L_2}\right)$$
$$+\hat{W}'''_{2n}(L_1)\left(\frac{L_2}{\omega_n}\right)^3 T\left(\frac{\omega_n x}{L_2}\right)+\frac{M_0}{m_0}\,\omega_n T\left[\frac{\omega_n(x-\xi)}{L_2}\right]H(x-\xi), \quad (14)$$

where $\hat{W}_{2n}(L_1)$, $\hat{W}'_{2n}(L_1)$, $\hat{W}''_{2n}(L_1)$, and $\hat{W}'''_{2n}(L_1)$ will be determined from the boundary conditions. To obtain these values, we need to look at section 1. As with the displacement, w_2, we will assume a separable solution for w_1. The spatial displacement and shear strain functions in the first section of the beam are assumed in the following form:

$$\bar{w}_{1n}(x)=\sum_{i=1}^{8}\bar{A}_{ni}\,e^{k^*_{ni}x} \quad (15)$$

$$\gamma_{c1n}(x)=\sum_{i=1}^{8}f_{ni}\bar{A}_{ni}\,e^{k^*_{ni}x} \quad (16)$$

$$\gamma_{c2n}(x)=\sum_{i=1}^{8}g_{ni}\bar{A}_{ni}\,e^{k^*_{ni}x} \quad (17)$$

where

$$f_{ni}=\frac{d_{23}d_{31}-d_{21}d_{33}}{d_{22}d_{33}-d_{32}d_{23}}$$

$$g_{ni}=\frac{d_{21}d_{32}-d_{22}d_{31}}{d_{22}d_{33}-d_{32}d_{23}}$$

$$d_{11}=-m\Omega_n^{*2}+(D+E_1A_1B_7^2+E_3A_3B_4^2+E_4A_4B_5^2)k_{ni}^{*4}$$

$$d_{12}=+(E_1A_1B_2B_7-E_3A_3B_4B_8+E_4A_4B_2B_5)h_{c1}k_{ni}^{*3}$$

$$d_{13}=(-E_1A_1B_3B_7-E_3A_3B_3B_4+E_4A_4B_5B_6)h_{c2}k_{ni}^{*3}$$

$$d_{21}=(E_1A_1B_2B_7-E_3A_3B_4B_8+E_4A_4B_2B_5)h_{c1}k_{ni}^{*3}$$

$$d_{22}=(B_2^2E_1A_1+B_8^2E_3A_3+B_2^2E_4A_4)h_{c1}^2k_{ni}^{*2}-G_{c1}A_{c1}$$

$$d_{23}=(-E_1A_1B_2B_3+E_3A_3B_3B_8+E_4A_4B_2B_6)h_{c1}h_{c2}k_{ni}^{*2}$$

$$d_{31}=(E_4A_4B_5B_6-E_1A_1B_3B_7-E_3A_3B_3B_4)h_{c2}k_{ni}^{*3}$$

$$d_{32}=(E_3A_3B_3B_8-E_1A_1B_2B_3+E_4A_4B_2B_6)h_{c1}h_{c2}k_{ni}^{*2}$$

$$d_{33}=(E_1A_1B_3^2+E_3A_3B_3^2+E_4A_4B_6^2)h_{c2}^2k_{ni}^{*2}-G_{c2}A_{c2}$$

and E_i, B_i and A_i are as defined in the Nomenclature.

According to the results found in Levy and Chen (1994), the characteristic equation for section 1 is expressed as

$$\det\begin{bmatrix}\bar{a}_{11} & \bar{a}_{12} & \bar{a}_{13}\\ \bar{a}_{21} & \bar{a}_{22} & \bar{a}_{23}\\ \bar{a}_{31} & \bar{a}_{32} & \bar{a}_{33}\end{bmatrix}=0, \tag{18}$$

where

$$\begin{aligned}
\bar{a}_{11} &= -m\Omega_n^{*2}+(D+E_1A_1B_7^2+E_3A_3B_4^2+E_4A_4B_5^2)k_n^{*4}\\
\bar{a}_{12} &= +(E_1A_1B_2B_7-E_3A_3B_4B_8+E_4A_4B_2B_5)h_{c1}k_n^{*3}\\
\bar{a}_{13} &= (-E_1A_1B_3B_7-E_3A_3B_3B_4+E_4A_4B_5B_6)h_{c2}k_n^{*3}\\
\bar{a}_{21} &= (E_1A_1B_2B_7-E_3A_3B_4B_8+E_4A_4B_2B_5)h_{c1}k_n^{*3}\\
\bar{a}_{22} &= (B_2^2E_1A_1+B_8^2E_3A_3+B_2^2E_4A_4)h_{c1}^2k_n^{*2}-G_{c1}A_{c1}\\
\bar{a}_{23} &= (-E_1A_1B_2B_3+E_3A_3B_3B_8+E_4A_4B_2B_6)h_{c1}h_{c2}k_n^{*2}\\
\bar{a}_{31} &= (E_4A_4B_5B_6-E_1A_1B_3B_7-E_3A_3B_3B_4)h_{c2}k_n^{*3}\\
\bar{a}_{32} &= (E_3A_3B_3B_8-E_1A_1B_2B_3+E_4A_4B_2B_6)h_{c1}h_{c2}k_n^{*2}\\
\bar{a}_{33} &= (E_1A_1B_3^2+E_3A_3B_3^2+E_4A_4B_6^2)h_{c2}^2k_n^{*2}-G_{c2}A_{c2}.
\end{aligned}$$

In the same manner, as in Levy and Chen (1994), the various boundary conditions and continuity conditions may be expressed:

at $x=0$:

$$\sum_{i=1}^{8}\bar{A}_{ni}k_{ni}^{*}=0 \tag{19}$$

$$\sum_{i=1}^{8}\bar{A}_{ni}=0 \tag{20}$$

$$\sum_{i=1}^{8}f_{ni}\bar{A}_{ni}=0 \tag{21}$$

$$\sum_{i=1}^{8}g_{ni}\bar{A}_{ni}=0 \tag{22}$$

at $x=L_1$:

The moment balance at the interface, as viewed from section 1, leads to the following:

$$\begin{aligned}
&\sum_{i=1}^{8}(D+E_1A_1B_7^2+E_3A_3B_4^2+E_4A_4B_5^2)\bar{A}_{ni}k_{ni}^{*2}\,e^{k_{ni}^{*}L_1}\\
&\quad+\sum_{i=1}^{8}(E_1A_1B_2B_7-E_3A_3B_4B_8+E_4A_4B_2B_5)h_{c1}f_{ni}\bar{A}_{ni}k_{ni}^{*}\,e^{k_{ni}^{*}L_1}\\
&\quad+\sum_{i=1}^{8}(E_4A_4B_5B_6-E_1A_1B_3B_7-E_3A_3B_3B_4)h_{c2}g_{ni}\bar{A}_{ni}k_{ni}^{*}\,e^{k_{ni}^{*}L_1}+M_2=0.
\end{aligned} \tag{23}$$

The moment balance at the interface, as viewed from section 2, leads to

$$D_{t1}\left[\hat{W}_{2n}(L_1)\left(\frac{\omega_n}{L_2}\right)^2 S\left(\frac{\omega_n L_1}{L_2}\right)+\hat{W}'_{2n}(L_1)\left(\frac{\omega_n}{L_2}\right)T\left(\frac{\omega_n L_1}{L_2}\right)\right.$$
$$\left.+\hat{W}''_{2n}(L_1)U\left(\frac{\omega_n L_1}{L_2}\right)+\hat{W}'''_{2n}(L_1)\left(\frac{L_2}{\omega_n}\right)V\left(\frac{\omega_n L_1}{L_2}\right)\right]+M_2=0. \quad (24)$$

The shear force balance at the interface, as viewed from section 1, leads to the following:

$$\sum_{i=1}^{8}(D+E_1A_1B_7^2+E_3A_3B_4^2+E_4A_4B_5^2)\bar{A}_{ni}k_{ni}^{*3}\,e^{k_{ni}^* L_1}$$
$$+\sum_{i=1}^{8}(E_1A_1B_2B_7-E_3A_3B_4B_8+E_4A_4B_2B_5)h_{c1}f_{ni}\bar{A}_{ni}k_{ni}^{*2}\,e^{k_{ni}^* L_1}$$
$$+\sum_{i=1}^{8}(E_4A_4B_5B_6-E_1A_1B_3B_7-E_3A_3B_3B_4)h_{c2}g_{ni}\bar{A}_{ni}k_{ni}^{*2}\,e^{k_{ni}^* L_1}-S_2=0. \quad (25)$$

The shear force balance at the interface, as viewed from section 2, leads to

$$D_{t1}\left[\hat{W}_{2n}(L_1)\left(\frac{\omega_n}{L_2}\right)^3 V\left(\frac{\omega_n L_1}{L_2}\right)+\hat{W}'_{2n}(L_1)\left(\frac{\omega_n}{L_2}\right)^2 S\left(\frac{\omega_n L_1}{L_2}\right)\right.$$
$$\left.+\hat{W}''_{2n}(L_1)\left(\frac{\omega_n}{L_2}\right)T\left(\frac{\omega_n L_1}{L_2}\right)+\hat{W}'''_{2n}(L_1)U\left(\frac{\omega_n L_1}{L_2}\right)\right]+S_2=0. \quad (26)$$

The equilibrium of the moment generated by the shear of each of the two damping layers is given by the following two equations:

$$\sum_{i=1}^{8}(E_3A_3B_4B_8-E_1A_1B_2B_7-E_4A_4B_2B_5)h_{c1}\bar{A}_{ni}k_{ni}^{*2}\,e^{k_{ni}^* L_1}-\sum_{i=1}^{8}(B_2^2E_1A_1+E_3A_3B_8^2$$
$$+E_4A_4B_2^2)h_{c1}^2f_{ni}\bar{A}_{ni}k_{ni}^{*}\,e^{k_{ni}^* L_1}+\sum_{i=1}^{8}(E_1A_1B_2B_3-E_3A_3B_3B_8$$
$$-E_4A_4B_2B_6)h_{c1}h_{c2}g_{ni}\bar{A}_{ni}k_{ni}^{*}\,e^{k_{ni}^* L_1}=0; \quad (27)$$

$$\sum_{i=1}^{8}(E_1A_1B_3B_7+E_3A_3B_3B_4-E_4A_4B_5B_6)h_{c2}\bar{A}_{ni}k_{ni}^{*2}\,e^{k_{ni}^* L_1}-\sum_{i=1}^{8}(E_1A_1B_2B_3-E_3A_3B_3B_8$$
$$+E_4A_4B_2B_6)h_{c1}h_{c2}f_{ni}\bar{A}_{ni}k_{ni}^{*}\,e^{k_{ni}^* L_1}-\sum_{i=1}^{8}(E_1A_1B_3^2+E_3A_3B_3^2$$
$$+E_4A_4B_6^2)h_{c2}^2g_{ni}\bar{A}_{ni}k_{ni}^{*}\,e^{k_{ni}^* L_1}=0 \quad (28)$$

at $x = L$:

The zero moment and transverse force conditions become

$$\hat{W}_{2n}(L_1)\left(\frac{\omega_n}{L_2}\right)^2 S\left(\frac{\omega_n L}{L_2}\right)+\hat{W}'_{2n}(L_1)\left(\frac{\omega_n}{L_2}\right)T\left(\frac{\omega_n L}{L_2}\right)$$
$$+\hat{W}''_{2n}(L_1)U\left(\frac{\omega_n L}{L_2}\right)+\hat{W}'''_{2n}(L_1)\left(\frac{L_2}{\omega_n L}\right)V\left(\frac{\omega_n L}{L_2}\right)=0 \quad (29)$$

$$\hat{W}_{2n}(L_1)\left(\frac{\omega_n}{L_2}\right)^3 V\left(\frac{\omega_n L}{L_2}\right)+\hat{W}'_{2n}(L_1)\left(\frac{\omega_n}{L_2}\right)^2 S\left(\frac{\omega_n L}{L_2}\right)$$
$$+\hat{W}''_{2n}(L_1)\left(\frac{\omega_n}{L_2}\right)T\left(\frac{\omega_n L}{L_2}\right)+\hat{W}'''_{2n}(L_1)U\left(\frac{\omega_n L}{L_2}\right)+\frac{M_0}{m_0}\frac{\omega_n^4}{L_2^2}=0. \quad (30)$$

The other two supplementary conditions representing the equilibrium of the axial forces in the constraining layers are

$$E_3A_3\frac{\partial u_3}{\partial x}=0 \quad (31a)$$

$$E_4A_4\frac{\partial u_4}{\partial x}=0. \quad (31b)$$

They may be written as

$$\sum_{i=1}^{8}\left(B_4k_{ni}^{*2}\,e^{k_{ni}^*L_1}-B_8h_{c1}f_{ni}k_{ni}^*\,e^{k_{ni}^*L_1}-B_3h_{c2}g_{ni}k_{ni}^*\,e^{k_{ni}^*L_1}\right)=0 \quad (32a)$$

$$\sum_{i=1}^{8}\left(B_8k_{ni}^{*2}\,e^{k_{ni}^*L_1}+B_2h_{c1}f_{ni}k_{ni}^*\,e^{k_{ni}^*L_1}+B_6h_{c2}g_{ni}k_{ni}^*\,e^{k_{ni}^*L_1}\right)=0. \quad (32b)$$

We can eliminate M_2 and S_2 from the above equations by combining eqns (23) and (24), and eqns (25) and (26). Hence, we have a total of 14 equations to determine the unknowns. In the above equations, if $M_0=0$, then the equations reduce to the case of the double sandwich-type cantilever with no mass at the free end. Equations (13) and (18)–(32) are nonlinear, complex valued equations for unknowns, Ω_n^*. A numerical scheme was used to obtain the results shown below. The uncovered cantilever beam with tip mass provided starting values for the scheme. These starting values and the secant method were employed to solve for Ω_n^*. By assuming a complex frequency factor, p^*, the real frequency factor (or the resonant frequency) p, and the loss factor η, of the beam are related to Ω_n^* by

$$\begin{aligned} p^* &= \Omega^* t_0 = p(1+j\eta)^{1/2} \\ p &= \Omega t_0 = \sqrt{\mathrm{Re}\,(p^{*2})} \\ \eta &= \mathrm{Im}\,(p^{*2})/\mathrm{Re}\,(p^{*2}) \end{aligned} \quad (33)$$

where $t_0=\sqrt{mL^4/D}$, m is the mass per unit length of section 1 and D is the effective bending stiffness of section 1, i.e. $\sum_{i=1,3,4}(E_ih_i^3)b/12$.

NUMERICAL RESULTS

Numerical results for the various mass ratios were obtained and are displayed as graphs. The input parameters employed in the previously described numerical scheme were the material and geometrical properties, mass density and core loss factor. The values chosen for the computation, unless stated otherwise, were

$$E_1 = E_3 = E_5 = 20.6 \times 10^{10}\,\mathrm{N/m^2};\quad G_{c1} = G_{c2} = 0.42 \times 10^8\,\mathrm{N/m^2};\quad L = 0.5\,\mathrm{m}, h_1 = 0.02\,\mathrm{m};$$

$$\rho_1 = \rho_3 = \rho_4 = 7850\,\mathrm{kg/m^3};\quad \rho_{c1} = \rho_{c2} = 3140\,\mathrm{kg/m^3};\quad h_3 = h_4 = h_{c1} = h_{c2} = 1/2h_1.$$

Mass ratio versus resonant frequency

Figure 2 shows the lowest resonant frequency versus the mass ratio (the attached mass to the mass of the beam). It can be observed that the increase in mass ratio will decrease the value of the lowest resonant frequency of the beam. This occurs because the increase in end mass causes the system to execute larger periodic excursions, increasing the period of oscillation, and hence, decreasing the frequency of oscillation. Also, the increase in the damping and constraining layer length will increase the value of the resonant frequency of the beam at constant mass ratio. This latter effect is the same as that obtained by Levy and Chen. This occurs, in this case, because the constraining layer values of E_3 and E_4 are the same as E_1, and the shear moduli are much smaller in magnitude. This has the effect of moving the cantilever end of the beam to L_1, thereby shortening the effective length of the beam. This, of course, increases the resonant frequency. It must be noted that the results are highly dependent on the input data and that the figures may have different trends for other input parameters.

Figure 3 represents the effect of mass ratio to the resonant frequency ratio. The mass ratio is as defined previously. The frequency ratio is that for the partially covered sandwich cantilever with mass of the free end to the resonant frequency of undamped cantilever beam without end mass. It can be seen that the increase in mass ratio will decrease the value of the frequency ratio and, hence, the resonant frequency. This coincides with Fig. 2 because in this case the resonant frequency of the undamped beam does not vary with end mass.

The effect of mass ratio to another definition of the resonant frequency ratio is given in Fig. 4. Here the frequency ratio is that of the partially covered sandwich cantilever with end mass compared to an undamped cantilever beam with mass at the free end. The frequencies that are compared are for the same mass ratio. For small mass ratio, the increase of mass ratio will decrease the resonant frequency ratio. For large mass ratio, the increase of mass ratio will increase the resonant frequency ratio. This may be explained as follows. For small mass ratio, the end mass plays a more important role to the damped beam than to the undamped beam, causing a decrease in the resonant frequency ratio. However, for large mass ratio, even though the large end mass causes a larger resonant frequency, the sandwich structure dominates and acts as if the fixed end of the beam is moved to the right, thus increasing the resonant frequency ratio of the sandwich beam compared to the uncovered beam with end mass.

From Figs 3 and 4 we note that, under certain circumstances, the covered beam will have a lower resonant frequency when an end mass is added (i.e. when a robot arm picks up a remote mass in its end effector) than an uncovered beam without end mass (i.e. an

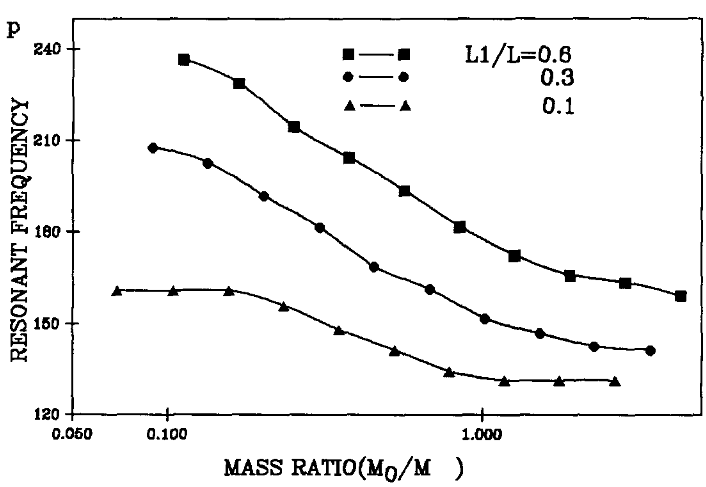

Fig. 2. Variations of resonant frequency versus mass ratio for various coverage lengths.

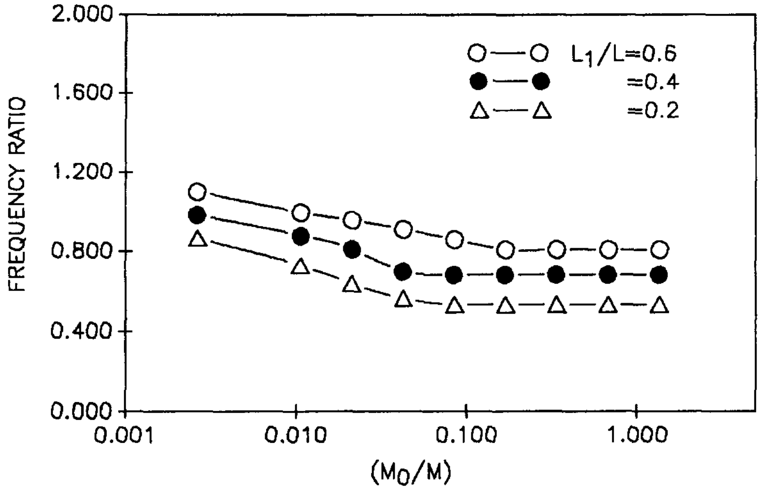

Fig. 3. Frequency ratio versus mass ratio for various coverage lengths related to an uncovered beam without end mass.

undamped robot arm without a mass in its end effector, Fig. 3). Also, the addition of damping material can reduce the resonant frequency (Fig. 4, $L_1/L = 0.4$ for M_0/M between 0.002 and 0.6) when compared to an uncovered beam having the same mass ratio. This indicates that small to moderate damping coverage may be counterproductive and one must be sensitive to this possibility.

Figure 5 represents the effect of mass ratio to the ratio of the second mode of resonant frequency. Here, the ratio is defined as the second resonant mode of the partially covered sandwich cantilever beam with end mass compared to the second resonant mode of an undamped cantilever beam with end mass. It may be seen that the increase of mass ratio will increase the resonant frequency ratio, i.e. sandwich structure dominates, and that coverage length plays no distinguishing role past $M_0/M = 0.1$. From the three figures (Figs 3–5), it appears that L_1/L should be greater than 0.4 to get good use of the damping coverage.

System loss factor versus damping coverage

Figure 6 represents the system loss factor versus the damping coverage. Here the core loss factor, η_{c1}, is taken as 1 to simplify the calculations. It may be seen from the figure that an increase in damping coverage will increase the system loss factor. The system loss factor

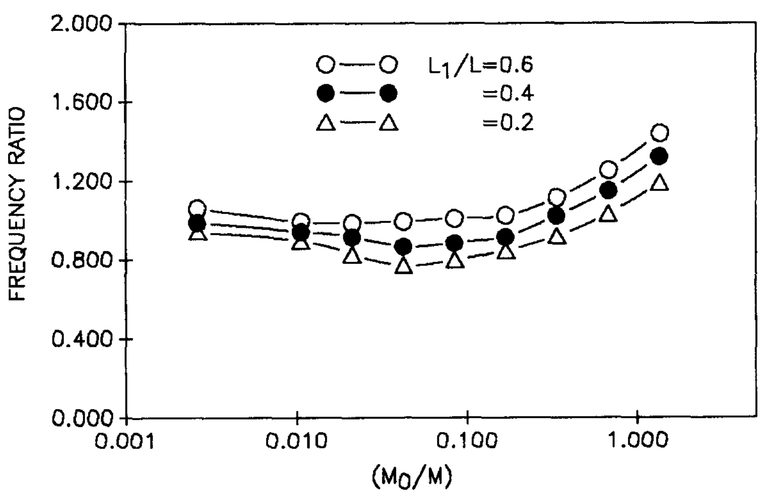

Fig. 4. Frequency ratio versus mass ratio for various coverage lengths related to an uncovered beam with end mass.

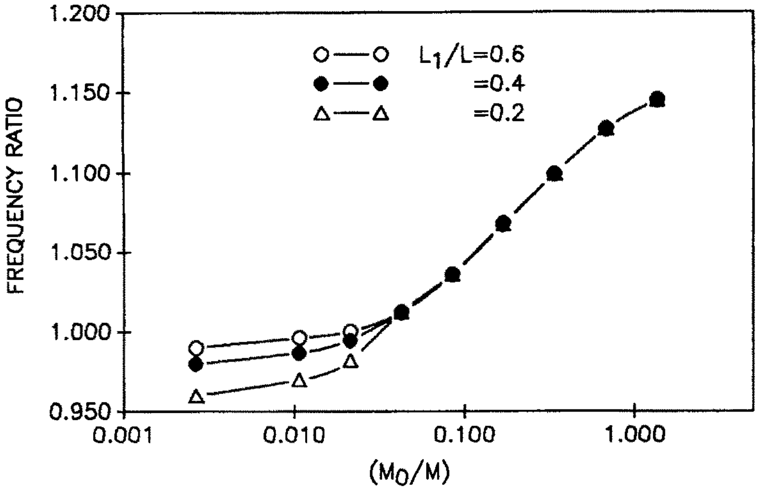

Fig. 5. Second mode resonant frequency ratio versus mass ratio for various coverage lengths related to an uncovered beam with end mass.

is related to energy dissipation. As more damping material covers the beam, more energy is dissipated, thus increasing the system loss factor.

An increase of the concentrated mass will also decrease the value of the system loss factor at constant coverage ratios. When the concentrated mass is very small compared to the mass of the beam, the increase of L_1/L will increase the value of the system loss factor. When the concentrated mass is large, the increase of L_1/L will decrease the value of the system loss factor. As more of the beam is covered the system loss factor increases once more. This may be explained as follows. The system loss factor is related to energy loss and the energy of such a viscoelastic system is dependent on the resonant frequency and transverse displacement of the system. For small mass, the vibrations of the beam are damped as the coverage, L_1/L, is increased; hence there is an increase in system loss factor. For constant coverage, as mass is added to the free end of the system, the beam must execute larger displacements. Hence, adding mass is equivalent to a reduction of the damping effect of the coverage and decreasing energy loss, thus a lower system loss factor. After some point, additional damping coverage counters the effect of the increase in mass. These explanations are consistent with the formula for a single degree of freedom viscoelastic system (Rao, 1990).

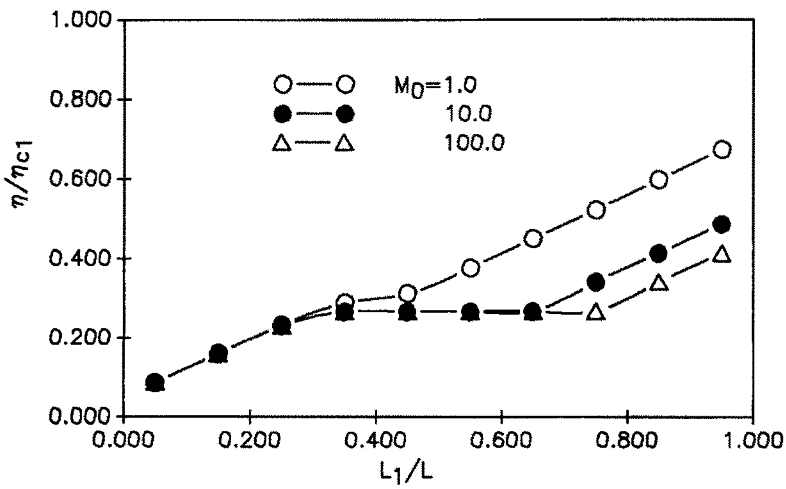

Fig. 6. Variation of system loss factor with damping coverage and mass.

System loss factor versus core shear modulus

The effects of core shear modulus with $L_1/L = 0.2$ are shown in Fig. 7. As can be seen, the system loss factor varies with the shear modulus (G_{c1} or G_{c2}). If the shear modulus is small, the increase of G_{c1} (or G_{c2}) will increase the system loss factor. After some point, if G_{c1} (or G_{c2}) continues to increase, the system loss factor will decrease. Thus, an optimal core shear modulus exists and the trend seen in this figure compares well with the results of Rao (1977, 1978). The optimal value of the core shear modulus is dependent on the system's geometrical and physical parameters. The form of the graph may be explained as follows. For small values of core shear modulus, the increase of core shear modulus will increase the core layer resistance and the energy dissipated, thus increasing the system loss factor. For very large core shear modulus, the damping factor is like the primary beam or the constraining layer, the relative deformation is very small, thus very little energy dissipation occurs. In this case, the loss factor is small. Between the two cases, there exists a value of G_{c1} or G_{c2}, which results in relatively large shear deformations and a large damping force leading to large energy dissipation. Hence, an optimal shear modulus exists. The addition of the end mass acts to counteract the effect of increasing G_c. As more mass is added, the loss factor decreases (consistent with the results in Fig. 2). Hence, the increase in mass has the overall tendency of decreasing the system loss factor.

Normally, the material properties of damping layers (elastic and shear modulus, loss factor) are functions of temperature and will affect the resonant frequency of the structure. But if the temperature is not changed very much or very fast (for example, a robot arm working at room temperature surroundings), we may consider the material properties to be constant to temperature. However, the results obtained here may be used to determine the correct value, if temperature variations are not large. For example, for a new temperature, a new G_c may be obtained using the manufacturer's specifications for which the system loss factor may be obtained from Fig. 7. This loss factor may be used in Fig. 6 to obtain the "apparent damping coverage" for a given M_0. The application of Fig. 6 defines an equivalent system with new coverage length having the same loss factor as the initial system with the new G_c but with the same M_0, all other parameters unchanged. This "apparent" damping coverage may be used in Fig. 2 to find the new resonant frequency for the new mass ratio of the equivalent system.

CONCLUSIONS

In this paper, the differential equations of motion governing the partially covered, double sandwich-type cantilever with concentrated mass at the free end were obtained and employed to find the resonant frequency and loss factor of the system. Data obtained for the resonant frequency and system loss factor are found to be highly dependent on the

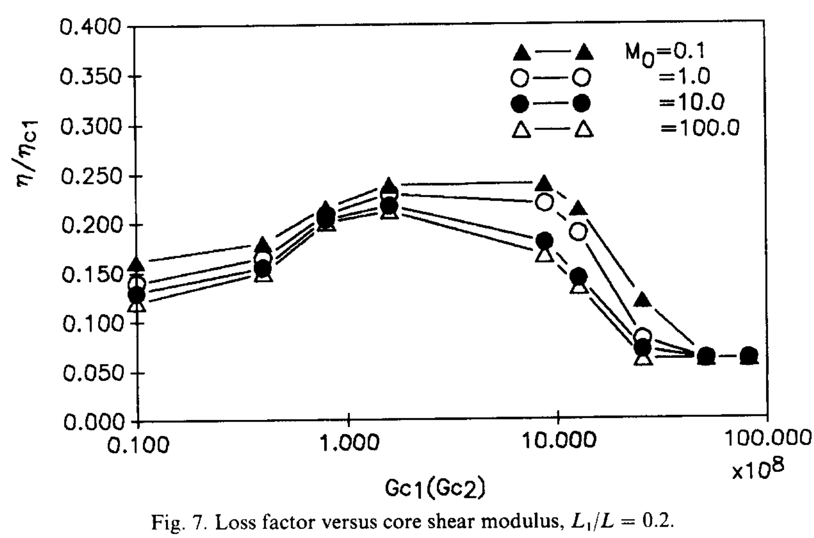

Fig. 7. Loss factor versus core shear modulus, $L_1/L = 0.2$.

input parameters. The following conclusions were obtained for our parameters: (1) an increase in mass ratio will decrease the resonant frequency; (2) an increase in damping coverage will increase the value of the system loss factor, but for certain coverages an increase of the mass ratio may cause a decrease in or flatten the value of the system loss factor; (3) after some large value of the coverage, the system loss factor will increase again; (4) there exists an optimal G_{c1} (or G_{c2}) whose value varies with different geometrical and physical parameters; (5) an optimum value of damping coverage exists for which the resonant frequency of the system is increased for both the first and second modes of vibration when compared, respectively, to the first and second modes of vibration of an uncovered beam with end mass.

REFERENCES

Amba-Rao, C. L. and Hussaini, M. Y. (1975). On free vibration of finite beams with partially fixed end conditions carrying masses. *J. Appl. Mech.* **42**(3), 735–736.

Chen, Q. (1986). Noise and vibration control of damped sandwich beams. Master's Thesis, Zhejiang University, People's Republic of China.

Ditaranto, R. A. (1965). Theory of vibratory bending for elastic and visco-elastic layered finite length beams. *J. Appl. Mech.* **87,** 881–886.

Gurgoze, M. (1986). On the approximate determination of the fundamental frequency of a restrained cantilever beam carrying a tip heavy body. *J. Sound Vibr.* **105,** 443–449.

Lall, A. K., Asnani, N. T. and Nakra, B. C. (1988). Damping analysis of partially covered sandwich beams. *J. Sound Vibr.* **123,** 247–259.

Laura, P. A. A., Susemihl, E. A., Pombo, J. L., Liusoni, L. E. and Gelos, R. (1977). On the dynamic behavior of structural elements carrying elastically mounted, concentrated masses. *Appl. Acoustics* **10,** 121–145.

Laura, P. A. A., Filipich, C. P. and Cortinez, V. H. (1987). Vibrations of beams and plates carrying concentrated masses. *J. Sound Vibr.* **117,** 459–465.

Levy, C. and Chen, Q. (1994). Vibration analysis of the partially covered double sandwich-type cantilever beam. *J. Sound Vibr.* In press.

Magrab, E. B. (1979). *Vibrations of Elastic Structural Members.* Sijthoff and Noordhoff International Publications B.V., The Netherlands.

Mead, D. J. and Markus, S. (1969). The forced vibration of a three-layer damped sandwich beam with arbitrary boundary conditions. *J. Sound Vibr.* **10,** 163–175.

Pan, H. H. (1965). Transverse vibration of an Euler beam carrying a system of heavy bodies. *J. Appl. Mech.* **32**(2), 434–437.

Rami Reddy, K. and Amba-Rao, C. L. (1973). Vibrations of beams carrying masses-transfer matrices approach. *J. Aero. Soc. India* **25**(3), 107–110.

Rao, D. K. (1977). Vibrations of short sandwich beams. *J. Sound Vibr.* **52**(2), 253–263.

Rao, D. K. (1978). Frequency and loss factors of sandwich beams under various boundary conditions. *J. Mech. Engng Sci.* **20**(5), 271–282.

Rao, S. S. (1990). *Mechanical Vibrations*, Chap. 8. Addison-Wesley, New York.

Stokey, W. F. and Zorowski, C. F. (1959). Normal vibrations of a uniform plate carrying any number of finite masses. *J. Appl. Mech.* **81,** 210–216.

Yan, M. J. and Dowell, E. H. (1972). Governing equations for vibrating constrained-layer damping sandwich plates and beams. *J. Appl. Mech.* **39,** 1041–1046.